The PI3K regulatory subunits p55α and p50α regulate cell death *in vivo*

Sara Pensa[1], Kevin Neoh[1], Henrike K Resemann[1], Peter A Kreuzaler[1,2], Kathrine Abell[1,3], Neil J Clarke[4], Thomas Reinheckel[5], C Ronald Kahn[6] and Christine J Watson[1*]

[1]Department of Pathology and [2]Department of Biochemistry, University of Cambridge, Tennis Court Road, Cambridge CB2 1QP, UK; [3]LEO Pharma A/S Industriparken 55, Ballerup DK-2750, Denmark; [4]GlaxoSmithKline, Gunnels Wood Road, Stevenage SG1 2NY, UK; [5]Institute of Molecular Medicine and Cell Research and BIOSS Centre for Biological Signalling Studies, Albert-Ludwigs-University Freiburg, Freiburg, Germany; [6] Joslin Diabetes Center, One Joslin Place, Boston MA 02215, USA

*Corresponding author

email: cjw53@cam.ac.uk

phone: +44 (0) 1223 333725

fax: +44 (0) 1223 333346

Running title

p55α and p50α regulate cell death

Keywords

p55α/p50α; cell death; mammary gland; cathepsin L; Stat3.

Abbreviations

LM-PCD, lysosomal-mediated programmed cell death; PI3Ks, phosphatidylinositol 3-kinases; SH2, Src homology 2**;** RTKs, receptor tyrosine kinases; SH3, Src homology 3; BH, breakpoint cluster region-homology; PTEN, phosphatase and tensin homolog; XBP-1, X-box-binding protein-1; UPR, unfolded protein response; ER, endoplasmic reticulum; Stat3, signal transducer and activator of transcription 3; LMP, lysosomal membrane permeabilisation; APR, acute phase response

SUMMARY

The PI3 Kinase regulatory subunits p55α and p50α are co-ordinately transcriptionally up-regulated by Stat3 at the onset of mammary gland involution, a process that requires Stat3. Deletion of both p55α and p50α subunits *in vivo* abrogated mammary epithelial cell death during involution. This was associated also with reduced cytosolic levels and activity of the cysteine protease cathepsin L, which is implicated in lysosomal-mediated programmed cell death (LM-PCD) and is upregulated in involution. Furthermore, involution is delayed in cathepsin L deficient mice suggesting that the p55α/p50α subunits mediate cell death in part by elevating the level of cathepsin L resulting in increased cytosolic activity. Surprisingly, we found that p55α/p50α localise to the nucleus where they bind to chromatin and regulate transcription of a subset of inflammatory/acute phase genes that are also Stat3 targets. Our findings reveal a novel role for these PI3K regulatory subunits as regulators of LM-PCD *in vivo*.

INTRODUCTION

The class IA phosphatidylinositol 3-kinases (PI3Ks) are heterodimeric enzymes that comprise a p110 catalytic subunit (p110α, p110β or p110δ) and a regulatory subunit (p85α, p85β, p55α, p55γ or p50α) [1]. A single gene, *pik3r1,* encodes p85α, p55α and p50α and all three subunits share a common carboxy-terminal domain which encompasses the p110 subunit binding site, a proline-rich region and two Src homology 2 (SH2) domains which bind to a plethora of proteins including receptor tyrosine kinases (RTKs) and ankyrin3 [2]. The unique amino terminal sequence of p85α comprises a Src homology 3 (SH3) and a breakpoint cluster region-homology (BH) domain which bind to the negative regulator of PI3K, phosphatase and tensin homolog (PTEN) enhancing its lipid phosphatase activity [3]. The p85α subunit binds also to Rab5 and other proteins including dynamin and Grb2 [2], and can interact with X-box-binding protein-1 (XBP-1), a transcriptional mediator of the unfolded protein response (UPR), to enhance nuclear accumulation of XBP-1s in an endoplasmic reticulum (ER) stress-dependent manner [4, 5]. The p55α and p50α subunits have much smaller unique N-terminal sequences of 34aa for p55α and 6aa for p50α. Specific ablation of these subunits by deleting exons 1B (p50α) and 1C (p55α) results in improved insulin sensitivity and protection from obesity-induced insulin resistance [6]. However, although p55α has been shown to bind to tubulin [7], the function of these subunits is still somewhat enigmatic.

Involution can be divided into two phases, the first of which is reversible [8]. In the mouse this reversible phase persists for approximately 48h and thereafter tissue remodelling occurs, precluding re-initiation of lactation. Gene expression analyses revealed an unexpected role for inflammatory regulators and the acute phase response during involution, reflecting the extensive tissue remodelling that occurs simultaneously with epithelial cell death [9-11]. We have shown previously that cell death during first phase involution is mediated by signal transducer and activator of transcription 3 (Stat3) regulated lysosomal membrane permeabilisation (LMP) and is independent of executioner caspases [12]. Furthermore, the lysosomal cathepsins B and L are strikingly upregulated during involution in a Stat3-

dependent manner and leak from lysosomes to initiate cell death. Thus, Stat3 is a master regulator of the involution process.

We demonstrated previously that transcription of p55α and p50α is specifically and dramatically upregulated by Stat3 at the onset of involution [13] and in a mammary epithelial cell line [14] and this prompted us to investigate their role in mediating the Stat3 signal during the involution process. Using mice in which the unique exons encoding the amino-termini of p55α and p50α were deleted, we found that mammary gland development occurred normally until involution, when cell death was dramatically reduced. The cysteine protease cathepsin L, which is implicated in lysosomal-mediated programmed cell death (LM-PCD), is rapidly upregulated in involution, although reduced cytosolic levels and activity are found in $p55\alpha^{-/-}/p50\alpha^{-/-}$ glands. Furthermore, cathepsin L deficient mice exhibited delayed involution suggesting that the p55α/p50α subunits mediate cell death in part by elevating cathepsin L activity. Interestingly, p55α/p50α localise to the nuclei of involuting epithelial cells and regulate transcription of a number of genes including some Stat3 target genes.

RESULTS

p55α/p50α regulate cell death *in vivo*

Examination of mammary glands from mice deficient in both p55α and p50α, but replete for p85α, revealed a striking delay in involution (Figure 1a and b). This was associated with delayed tissue remodelling, as shown by the quantification of the area occupied by adipocytes, which is significantly reduced at 48h and 72h of involution (Figure 1c). In addition, 24h involution samples show a 12-fold reduction in the number of detached dying cells (Figure 1b and d), also indicated by decreased cleaved caspase 3 levels (Figure 1e and f). Levels of p-Akt and phospho-Glycogen synthase kinase 3 β (p-Gsk3β) were similar between control and knockout mice except at 72h involution (Supplementary Figure 1a) due largely to the presence of Akt2 in the adipose tissue at this time point (Supplementary Figure 1b and 1c). Thus, the role of p55α/p50α during involution is likely

independent of PI3K catalytic activity. This suggests that these subunits have a role in regulating cell death during involution by some other mechanism. Notably, p55α/p50α expression in the mammary gland seems to be restricted to the epithelium and is not found in the adipose compartment (Supplementary Figure 1c).

p55α/p50α regulate cathepsin L expression and cytosolic activity

We have shown previously that, during involution, Stat3 upregulates expression of the lysosomal proteases cathepsins B and L while downregulating expression of the endogenous cathepsin inhibitor Spi2a [12]. Importantly, as opposed to cathepsin B, which shows a modest 4-fold increase at the onset of involution ([12] and Figure 3d), cathepsin L shows a striking induction within 24h involution, as shown by immunofluorescence staining and a corresponding 22-fold induction at the mRNA level (Figure 2a and 3d) and [12, 15]. We confirmed that cathepsin L localises to vesicles at 24h involution using immunofluorescence microscopy (Figure 2a). The discrete puncta observed become more diffuse as involution progresses and begin to disappear altogether at 96h, reflecting the reduction in cathepsin L compared to cathepsin B at this time point [12]. Interestingly we found that, while both cathepsins B and L normally co-localised, a proportion of the cathepsin L positive vesicles did not contain cathepsin B (Figures 2b and Supplementary figure 2) suggesting that there may be an alternative transport system that delivers cathepsin L to discrete vesicles. Importantly, ablation of p55α/p50α affected primarily cathepsin L levels, which were dramatically reduced in knockout tissue and this was particularly marked in the extent of cathepsin L leakage to the cytosol (Figures 2c and Supplementary figure 3a). In contrast, cathepsin B levels were relatively unchanged (Supplementary figure 3b-d). This was reflected in enzymatic activity assays on both lysosomal and cytosolic extracts, showing reduced cathepsin L cytosolic activity both at 24h and 48h involution (Figure 2d). Since cathepsin B activity is unaffected by p55α/p50α ablation, this suggests that lysosomal leakiness is unlikely to be perturbed. Therefore the reduced cytosolic activity of cathepsin L most likely reflects the reduced protein levels observed.

We have previously shown that the mitochondrial pathway of cell death is downstream of LM-PCD and is executioner caspase-independent [12]. Nevertheless we investigated whether deletion of p55α/p50α affected components of the mitochondrial pathway. Thus we analysed the expression of the pro-apoptotic Bcl-2 family members Bax and Bid and the anti-apoptotic factors Bcl-2 and Bcl-xL (Supplementary figure 4a). No major changes were observed, although slightly reduced cytosolic levels of cytochrome c were apparent at 48h involution in the *p55α*$^{-/-}$*/p50α*$^{-/-}$ glands (Supplementary figure 4b), suggesting an impact of cathepsin L on the mitochondria.

p55α/p50α regulate gene expression at the transcriptional and post-transcriptional level

Recently, p85α has been shown to interact with XBP-1 and regulate its nuclear translocation and transcriptional activity [4, 5]. We therefore sought to determine if p55α/p50α could exert a similar function on the master regulator of involution, Stat3. Analysis of total and nuclear extracts of *p55α*$^{-/-}$*/p50α*$^{-/-}$ glands at different involution time points revealed no difference in the induction of Stat3 phosphorylation or on its translocation to the nucleus (Supplementary figure 5a-c). Nuclear localisation of p85α and p85β has been described in different cellular systems [4, 16, 17]. To determine if the regulatory subunits localise to the nuclei of mammary cells, we analysed nuclear and cytosolic extracts of a number of involution time points. Interestingly, we detected nuclear p85α at 10 days lactation while p55α and p50α exhibited nuclear localization immediately upon their expression at the onset of involution (Figure 3a). Further analysis of nuclear compartments revealed an association of all three regulatory subunits, and p-Stat3, with chromatin-enriched extracts of the EpH4 mammary epithelial cells, suggesting either a direct or indirect role in regulating transcription (Figure 3b). This prompted us to carry out a microarray analysis of control and *p55α*$^{-/-}$*/p50α*$^{-/-}$ mammary glands at 24h of involution. A number of genes were either upregulated or downregulated in the *p55α*$^{-/-}$*/p50α*$^{-/-}$ glands (Supplementary tables 1 and 2 respectively) and a subset of these was validated by QRT-PCR (Figure 3c). Interestingly, a number of these genes are associated with cell migration and tissue remodelling and the acute phase response (APR). While osteopontin (Spp1), SAA2 and Tlr2 are expressed at higher levels in the absence of p55α/p50α, Slpi and Synaptopodin are suppressed in

p55α/p50α deficient glands. Many of the genes identified in the microarray have previously been shown to be Stat3 targets ([10] Supplementary Table 3 and CJW, unpublished,). This suggests that the regulatory subunits may fine-tune Stat3 regulated gene expression. However, transcription of Stat3 regulated genes implicated in LM-PCD, such as Spi2a and cathepsins B and L, was not affected by ablation of p55α/p50α although there was a trend of reduced expression of cathepsin L (Figure 3d). Taken together, these data suggest that p55α/p50α modulate the expression of distinct sets of genes at either the transcriptional or post-transcriptional level during mammary gland involution.

Cathepsin L is an important mediator of mammary gland involution.

The specific regulation of cathepsin L downstream of the small regulatory subunits p55α/p50α points to an important role for this lysosomal enzyme in cell death. To address this function directly, we investigated involution at various time points in cathepsin L null mice. Involution was markedly delayed with a 3-fold reduction in the extent of tissue remodelling observed in $ctsl^{-/-}$ mammary glands at 72h involution as measured by the area occupied by adipocytes (Figure 4a-c). In addition, perilipin staining of mammary glands at 72h of involution highlights the delayed reappearance of the adipocytes in the $ctsl^{-/-}$ glands when compared to the controls (Figure 4d).

DISCUSSION

Of the three subunits encoded by the *pi3kr1* gene, p85α has been implicated in a plethora of functions, which may be either PI3K dependent or independent and are exerted mainly through interaction with several binding partners in different contexts [18]. The role of the smaller p55α/p50α subunits is however still obscure. The only clearly defined function for p55α/p50α was revealed by their genetic deletion which resulted in increased insulin sensitivity, demonstrating a role for the small subunits in insulin signalling, particularly in glucose and lipid metabolism [6]. It has been hypothesised that their unique N-termini may target these subunits to different compartments of the cell, thus allowing for localised PI3K-dependent signalling events. For example, the p55α N-terminus has been shown to interact with tubulin, thus localising this subunit to the microtubule network [7].

Here we show that p55α/p50α, specifically upregulated at the onset of involution by Stat3, play a fundamental role *in vivo* by regulating mammary gland involution. In the absence of the small subunits, mammary gland involution is substantially delayed, with a severe effect on the levels of cell death during the early stages of this process (Figure 1). Surprisingly, p55α/p50α affect cell death independently of PI3K signalling, as phosphorylation of Akt and its downstream targets are largely unaffected in knockout tissue (Supplementary figure 1).

One mechanism by which the subunits influence cell death, which occurs by LM-PCD, is by upregulating levels of the lysosomal protease cathepsin L (Figure 2). Furthermore, we provide evidence that reduced activity of cathepsin L can at least partially account for the delay in involution observed in the p55α/p50α mice, since complete depletion of this lysosomal protease, as observed in *ctsl*$^{-/-}$ mice, is sufficient to delay mammary gland involution (Figure 4).

The upregulation of cathepsin L does not seem to occur directly through transcriptional regulation, as the mRNA levels of cathepsin L are not significantly reduced in the *p55α*$^{-/-}$*/p50α*$^{-/-}$ mice (Figure 3d). Post-transcriptional regulation of cathepsin L has not been investigated and could occur by alterations in mRNA stability or post-translational delivery to the lysosomal compartment.

Interestingly however, we could detect p55α/p50α, as well as p85α, in the nuclear compartment of mammary tissue and mammary cell lines (Figure 3a and b). There is some evidence in the literature for nuclear localisation of particular regulatory subunits of PI3K. For example, p85α has been shown to localise to the nuclei of both PC12 cells upon Haloperidol treatment [16] and C6 glial cells cultured in serum-free medium [17]. More recently, interaction of p85α or p85β with XBP-1s has been shown to increase nuclear localization of XBP-1s and transcriptional regulation of the unfolded protein response [4, 5]. Furthermore, both p85α and p85β have been shown to be present in nuclear preparations of mouse embryo fibroblasts [4]. Our finding that p55α/p50α localize to the nuclei of mammary cells and associate with chromatin, is the first demonstration of a potential nuclear function for these smaller subunits. This notion is supported by our microarray analysis demonstrating that gene expression during involution is modulated by depletion of p55α/p50α suggesting a role in

transcriptional regulation which could be mediated by influencing the activity of other transcription factors, such as Stat3 (Figure 3c and Supplementary Tables). However, further investigation is required to address the specific mechanism.

Mammary gland involution is associated with a dramatic upregulation of the APR and inflammatory genes [11, 14, 19]. The APR is a component of the innate immune system and the first mechanism of defence against disease, aimed at minimising tissue damage while promoting repair. We have recently demonstrated some of the APR genes to be transcriptional targets of Stat3 in the mammary gland [10], where they may act to ensure efficient tissue remodelling.

An initial comparison of the most dramatically p50α/p55α-regulated genes reveals that many downregulated targets are also substantially downregulated in the absence of Stat3. Similarly, many of the genes upregulated in the 24h p50α/p55α depleted mammary gland are also upregulated in the *Stat3*$^{-/-}$ tissue (Supplementary Table 3). These correlations indicate that a set of Stat3-regulated involution target genes are also regulated via p50α/p55α, suggesting that these subunits modulate the Stat3 signal. Intriguingly, however, a small number of genes are upregulated in the *p55α*$^{-/-}$*/p50α*$^{-/-}$ but downregulated in the *Stat3*$^{-/-}$glands, indicating positive regulation by Stat3 and negative regulation by p50α/p55α. The reason for this is not clear but may be a mechanism for fine-tuning the amplitude of the Stat3 response.

Our previous work demonstrated that Stat3 regulates LM-PCD [12] and induces expression of p55α and p50α [13]. In other work (Pensa et al, unpublished) we have shown that p55α and p50α regulate the autophagic flux during involution. We propose a novel function for these subunits as key players in determining the balance of tissue remodelling signals and cell death in the physiological context of mammary gland involution. This balance between autophagy and cell death is of crucial importance in many different biological processes. Thus, we anticipate that p55α/p50α may be central in cell fate decisions in other systems *in vivo* where they can regulate autophagy and cell death. The APR and the inflammatory response associated with involution have been recently demonstrated to provide a pro-tumorigenic microenvironment in the mammary gland [20]. In addition, deregulation of Stat3 target

genes can account for its pro-tumourigenic role as opposed to the pro-cell death role in normal tissue [21]. It would be interesting to investigate if the subunits could be responsible for such a switch in Stat3 function in pathological *versus* physiological conditions. The observation that p55α/p50α show higher levels in low grade as compared to aggressive neuroblastomas [22] and that transcription of p55α/p50α by Stat3 switches MEFs from a pro-survival to an anti-survival response to LIF [23] would support this hypothesis.

METHODS

Animal husbandry. *p50α/p55α* and *ctsl* null mice have been generated previously (respectively [6] and [24]). C57BL/6 mice were purchased from Harlan labs. The mice were bred in regular cages with food and water ad libitum. Virgin female mice, 8-14 weeks old, were mated and males were subsequently removed before birth to avoid second pregnancies. Dams were killed at indicated time points. For involution studies, pups were removed at 10 days of lactation. Unless otherwise stated, at least three mice were used for each time point in every experiment. All animals were treated according to local ethical committee and the UK Home Office guidelines and killed through CO2 asphyxiation or dislocation of the neck.

Assessment of delayed involution in vivo. To quantify the delay of mammary gland involution, the area occupied by adipocytes was assessed by analysis of haematoxylin- and eosin-stained mammary gland sections using ImageJ software.

Haematoxylin and eosin staining. Haematoxylin and eosin staining was carried out as previously described [25].

Adipocyte isolation. Pairs of cervical and abdominal (minus lymph nodes) glands were extracted, pooled and minced manually and a small amount of tissue was retained for extraction of total protein. The remaining material was digested for 1 h in 2.5 ml 3 mg/ml type II collagenase at 37^{o}C with shaking (200 rpm), followed by filtration (filter cap 100 mm pore size, BD Biosciences, CA, US) and

centrifugation at low speed (1300 rpm). After centrifugation, mature adipocytes on the surface of the digestion mixture were removed by pipette. 'Undigested' tissue (material that failed to pass through the filter mesh) containing epithelium, stroma, and some undigested fat, was retained for analysis. Pelleted material (1300 rpm), expected to contain pre-adipocytes, was also similarly retained.

Lysosomal subcellular fractionation. Lysosomal crude extracts were obtained as previously described [3]. Briefly, lymph node divested number four glands were homogenized in a tight-fitting handheld homogenizer in 1 ml of subcellular fractionation buffer (HEPES-KOH 20 mM, sucrose 250 mM, KCl 10 mM, MgCl2 1.5 mM, EDTA 1 mM, EGTA 1 mM, dithiothreitol 8 mM, Pefabloc 1mM (Sigma Aldrich, MO, US), at pH 7.5). Debris and nuclei were pelleted at 750g (3,500 r.p.m., Optima L-100 XP Ultracentrifuge, 4 C, BeckmanCoulter, CA, US) for 12 min. The supernatant was spun at 10,000g (12,900 r.p.m.) for 35 min to pellet lysosomes and other organelles. The pellet was rinsed and collected in 300 μl subcellular fractionation buffer as lysosomal fraction. The supernatant, containing cytosolic and extracellular components, was cleared of microsomes by an additional spin at 100,000g (40,000 r.p.m.) for 1 h and collected as cytosolic fraction. Three cycles of freezing and thawing were employed to disrupt the organelles.

Cathepsin B and L activity. To measure lysosomal and cytosolic cathepsin activity, subcellular fractionation was carried out as described earlier. Protein levels were assessed with the BCA Protein Assay (Thermo Fisher Scientific, MA, US) and equal amounts of protein (4 μg) were added to a total of 200 μl cathepsin reaction buffer (sodium acetate 50 mM, EDTA 8 mM, dithiothreitol 8mM and Pefabloc subcellular fractionation buffer 1 mM, at pH6). Cathepsin B+L activity was measured after incubation (15 min, 37C) with the fluorescent substrate Z- Phe-Arg-AMC (50 μM, Merk Millipore, Danmstadt, Germany) in a Synergy HT Multi-Detection Microplate Reader (excitation 380 nM, emission 442 nM, Bio-TEK, VT, US). In parallel, a sample with added cathepsin B inhibitor CA-074 (5 μM, Peptanova, Sandhausen, Germany) was measured to determine cathepsin L activity. The cathepsin B activity measurement was detracted from the difference between readings.

Cytosolic-nuclear fractionation. Cytosolic and nuclear fractions were prepared as following: frozen

tissue powder was resuspended in three pellet volumes of cold buffer A (20 mM HEPES, pH 7.0, 0.15 mM EDTA, 0.015 mM EGTA, 10 mM KCl, 1 mM phenylmethylsulfonyl fluoride, 20 mM NaF, 1 mM sodium pyrophosphate, 1 mM sodium orthovanadate, 1% Nonidet P-40, and protease inhibitors cocktail [Sigma]). The homogenate was centrifuged at 500 × g for 5 min. The supernatant corresponds to the cytosolic fraction. The nuclear pellet was resuspended in five pellet volumes of cold buffer B (10 mM HEPES, pH 8.0, 0.1 mM EDTA, 1 mM phenylmethylsulfonyl fluoride, 20 mM NaF, 1 mM sodium pyrophosphate, 1 mM sodium orthovanadate, 25% glycerol, 0.1 M NaCl, and protease inhibitors cocktail). After centrifugation the nuclei were resuspended in two pellet volumes of hypertonic cold buffer C (10 mM HEPES, pH 8.0, 0.1 mM EDTA, 1 mM phenylmethylsulfonyl fluoride, 20 mM NaF, 1 mM sodium pyrophosphate, 1 mM sodium orthovanadate, 25% glycerol, 0.4 M NaCl, and protease inhibitors cocktail) and were incubated for 30 min at 4 °C in a rotating wheel and nuclear debris were removed by centrifugation at 900 × g for 20 min at 4 °C.

Small scale chromatin-cytosolic fractionation. EpH4 cells were grown in DMEM (Life Technologies, CA, US) containing 10% foetal calf serum (FCS, Sigma). To isolate the chromatin, cells were plated in 10 cm dishes, treated with OSM for 24 hours, crosslinked and quenched as described before [26]. Cells were washed with PBS, centrifuged and the cell pellet was resuspended in buffer A (10 mM HEPES [pH 7.9], 10 mM KCl, 1.5 mM MgCl2, 0.34 M sucrose, 10% glycerol, 1 mM dithiothreitol, and protease inhibitor cocktail [Sigma]). Triton X-100 was added (0.1% final concentration), the cells were incubated on ice for 10 min, and nuclei were collected by centrifugation (5 min, 1,300 × *g*, 4°C). The supernatant constitutes the cytosolic fraction. The nuclei were washed once in buffer A and lysed for 30 min in buffer B (3 mM EDTA, 0.2 mM EGTA, 1 mM dithiothreitol, and protease inhibitor cocktail), and insoluble chromatin and soluble fraction were separated by centrifugation (5 min, 1,700 × *g*, 4°C). The chromatin fraction was washed five times with buffer B. On the last wash, sonication was performed for 30 seconds. After centrifugation at 4,000 rpm 5 minutes 4ºC, the chromatin pellet was resuspended in 55 µl 1X DNase I Buffer + 5 µl DNase (Promega, WI, US), incubated at 37°C for 30-60 minutes and boiled 15 minutes in sodium dodecyl sulphate (SDS) loading buffer.

Quantitative real-time PCR. RNA extraction, complementary DNA synthesis and quantitative real-time PCR were carried out as previously described[25]. Primers used were: *cyclophilin A* (housekeeping gene) forward, 5'-CCT TGG GCC GCG TCT CCT T-3', reverse, 5'-CAC CCT GGC ACA TGA ATC CTG-3'; *cathepsin B* forward, 5'-TCC TTG ATCC TTC TTT CTT GCC-3', reverse, 5'-ACA GTG CCA CAC AGC TTC TTC-3'; *cathepsin L* forward, 5'-ATC AAA CCT TTA GTG CAG AGT G-3', reverse, 5'-CTG TAT TCC CCG TTG TGT AGC-3'; *Spi2A* forward, 5'-TTT CCA GCA ACC TCT CAA GGC-3', reverse, 5'-CTG GGT GTG ATT GCC CAC ATA-3'. *Saa2* forward, 5'-TGGCTGGAAAGATGGAGACAA-3', reverse, 5'-AAAGCTCTCTCTTGCATCACTG-3'; *Spp1* forward, 5'-AGCAAGAAACTCTTCCAAGCAA-3', reverse, 5'-GTGAGATTCGTCAGATTCATCCG-3'; *Synpo* forward, 5'-GCTCATTGACATGCAGCCTA-3', reverse, 5'-GCCTTCTCTCCAAACTGTCG-3'; *Tlr2* forward, 5'-GCAAACGCTGTTCTGCTCAG-3', reverse, 5'-AGGCGTCTCCCTCTATTGTATT-3'. Primers were designed using the PrimerBank website (http://pga.mgh.harvard.edu/primerbank/).

Immunoblotting. Sample preparation and immunoblotting were carried out as previously described [25]. The following antibodies from Cell Signalling Technologies (MA, US) were used: anti-phospho-Stat3 (Tyr705: 9131), anti-total-Stat3 (9132), anti-phospho-Akt (Ser473: 9271), anti-total-Akt (9272), anti-phospho-Gsk3β (9331), anti-GSK3β (9315), anti-Akt1 (2967), anti-Akt2 (2964), anti-Akt3 (4059) and anti-Lamin A/C (2032). The following antibodies from Abcam (Cambridge, UK) were used: anti-cathepsin B (ab33538), anti-Lamp2 (ab13524), anti-Tubulin (ab6160) and anti-β-actin (ab8227). The following antibodies from Santa Cruz Biotechnology (CA, US) were used: anti-C/ebpα (sc-61), anti-histone H3 (sc8654), anti-Bax (sc-7480), anti-Bcl-2 (sc7382) and anti-Bcl-xL (sc-634). Other commercial antibodies used were: anti-cathepsin L (MAB9521), anti-cathepsin L (AF1515, used for the immunodetection of cathepsin L in the cathepsin L knockout and control glands) and anti-Bid (MB860) from R&D Systems (MN, US), anti-pan-p85 (Millipore, 06-496, also detects p50α/p55α subunits), anti-cytochrome c (65981A) and anti-E-cadherin (610182) from BD biosciences. All antibodies were used at a standard dilution of 1:1,000. Secondary horseradish peroxidase (HRP)-conjugated antibodies were purchased from Dako (Glostrup, Denmark).

Immunohistochemistry. Tissue sections were prepared as previously described [25]. For assessment of cathepsin localization on tissue sections, the tissue was permeabilized with 0.1% saponin (Sigma) in PBS and blocked in 10% normal goat serum (Dako) in PBS, 0.01% saponin. The pictures of c-C3 were acquired on a Zeiss Axioplan 2 microscope. All the other pictures were acquired on a Zeiss LSM 700 confocal microscope. z stacks for the cathepsin B and L costaining was carried out on at least five z stacks from two independent biological replicates with at least 10 cross-sections for every sample. Primary antibodies used were: rat anti-cathepsin L (R&D Systems, MAB9521, 1:200), rabbit anti-cathepsin B (Abcam, 1:100), mouse anti-E-cadherin (BD biosciences, 610182, 1:500), rabbit anti-perilipin (Cell Signalling, 3470, 1:200) and rabbit anti-cleaved Caspase 3 (Cell Signalling 9661, 1:100). Secondary antibodies used were Alexa Fluor 488 goat-anti-rabbit-IgG (Invitrogen, 1:500) Cy3 goat-anti-rabbit (Invitrogen, 1:500) and Cy3 goat-anti-rat-IgG (Invitrogen, 1:500). Nuclei were counterstained with Hoechst 33342 (Sigma, 1:1,000).

Statistical analysis. Every experiment was carried out with at least three independent biological samples. Where appropriate, statistical significance was assessed with Student's t -test.

REFERENCES

1. Vanhaesebroeck B, Ali K, Bilancio A, Geering B, Foukas LC. Signalling by PI3K isoforms: insights from gene-targeted mice. *Trends Biochem Sci* 2005 Apr; **30**(4)**:** 194-204.

2. Mellor P, Furber LA, Nyarko JN, Anderson DH. Multiple roles for the p85alpha isoform in the regulation and function of PI3K signalling and receptor trafficking. *Biochem J* 2012 Jan 1; **441**(1)**:** 23-37.

3. Chagpar RB, Links PH, Pastor MC, Furber LA, Hawrysh AD, Chamberlain MD*, et al.* Direct positive regulation of PTEN by the p85 subunit of phosphatidylinositol 3-kinase. *Proc Natl Acad Sci U S A* 2010 Mar 23; **107**(12)**:** 5471-5476.

4. Park SW, Zhou Y, Lee J, Lu A, Sun C, Chung J*, et al.* The regulatory subunits of PI3K, p85alpha and p85beta, interact with XBP-1 and increase its nuclear translocation. *Nat Med* 2010 Apr; **16**(4)**:** 429-437.

5. Winnay JN, Boucher J, Mori MA, Ueki K, Kahn CR. A regulatory subunit of phosphoinositide 3-kinase increases the nuclear accumulation of X-box-binding protein-1 to modulate the unfolded protein response. *Nat Med* 2010 Apr; **16**(4)**:** 438-445.

6. Chen D, Mauvais-Jarvis F, Bluher M, Fisher SJ, Jozsi A, Goodyear LJ*, et al.* p50alpha/p55alpha phosphoinositide 3-kinase knockout mice exhibit enhanced insulin sensitivity. *Mol Cell Biol* 2004 Jan; **24**(1)**:** 320-329.

7. Inukai K, Funaki M, Nawano M, Katagiri H, Ogihara T, Anai M*, et al.* The N-terminal 34 residues of the 55 kDa regulatory subunits of phosphoinositide 3-kinase interact with tubulin. *Biochem J* 2000 Mar 1; **346 Pt 2:** 483-489.

8. Watson CJ. Post-lactational mammary gland regression: molecular basis and implications for breast cancer. *Expert Rev Mol Med* 2006; **8**(32)**:** 1-15.

9. Chapman RS, Lourenco PC, Tonner E, Flint DJ, Selbert S, Takeda K*, et al.* Suppression of epithelial apoptosis and delayed mammary gland involution in mice with a conditional knockout of Stat3. *Genes Dev* 1999 Oct 1; **13**(19)**:** 2604-2616.

10. Hughes K, Wickenden JA, Allen JE, Watson CJ. Conditional deletion of Stat3 in mammary epithelium impairs the acute phase response and modulates immune cell numbers during post-lactational regression. *J Pathol* 2012 May; **227**(1)**:** 106-117.

11. Stein T, Morris JS, Davies CR, Weber-Hall SJ, Duffy MA, Heath VJ*, et al.* Involution of the mouse mammary gland is associated with an immune cascade and an acute-phase response, involving LBP, CD14 and STAT3. *Breast cancer research : BCR* 2004; **6**(2)**:** R75-91.

12. Kreuzaler PA, Staniszewska AD, Li W, Omidvar N, Kedjouar B, Turkson J*, et al.* Stat3 controls lysosomal-mediated cell death in vivo. *Nat Cell Biol* 2011 Mar; **13**(3)**:** 303-309.

13. Abell K, Bilancio A, Clarkson RW, Tiffen PG, Altaparmakov AI, Burdon TG*, et al.* Stat3-induced apoptosis requires a molecular switch in PI(3)K subunit composition. *Nat Cell Biol* 2005 Apr; **7**(4)**:** 392-398.

14. Clarkson RW, Boland MP, Kritikou EA, Lee JM, Freeman TC, Tiffen PG*, et al.* The genes induced by signal transducer and activators of transcription (STAT)3 and STAT5 in mammary epithelial cells define the roles of these STATs in mammary development. *Mol Endocrinol* 2006 Mar; **20**(3)**:** 675-685.

15. Burke MA, Hutter D, Reshamwala RP, Knepper JE. Cathepsin L plays an active role in involution of the mouse mammary gland. *Dev Dyn* 2003 Jul; **227**(3)**:** 315-322.

16. Dai Y, Wei Z, Sephton CF, Zhang D, Anderson DH, Mousseau DD. Haloperidol induces the nuclear translocation of phosphatidylinositol 3'-kinase to disrupt Akt phosphorylation in PC12 cells. *J Psychiatry Neurosci* 2007 Sep; **32**(5)**:** 323-330.

17. Sephton CF, Mousseau DD. Dephosphorylation of Akt in C6 cells grown in serum-free conditions corresponds with redistribution of p85/PI3K to the nucleus. *J Neurosci Res* 2008 Feb 15; **86**(3)**:** 675-682.

18. Mellor P, Furber LA, Nyarko JN, Anderson DH. Multiple roles for the p85alpha isoform in the regulation and function of PI3K signalling and receptor trafficking. *The Biochemical journal* 2012 Jan 1; **441**(1)**:** 23-37.

19. Pensa S, Watson CJ, Poli V. Stat3 and the inflammation/acute phase response in involution and breast cancer. *J Mammary Gland Biol Neoplasia* 2009 Jun; **14**(2)**:** 121-129.

20. Lyons TR, O'Brien J, Borges VF, Conklin MW, Keely PJ, Eliceiri KW*, et al.* Postpartum mammary gland involution drives progression of ductal carcinoma in situ through collagen and COX-2. *Nature medicine* 2011 Sep; **17**(9)**:** 1109-1115.

21. Resemann HK, Watson CJ, Lloyd-Lewis B. The Stat3 paradox: A killer and an oncogene. *Mol Cell Endocrinol* 2013 Jul 1.

22. Fransson S, Kogner P, Martinsson T, Ejeskar K. Aggressive neuroblastomas have high p110alpha but low p110delta and p55alpha/p50alpha protein levels compared to low stage neuroblastomas. *J Mol Signal* 2013; **8**(1)**:** 4.

23. Lu Y, Fukuyama S, Yoshida R, Kobayashi T, Saeki K, Shiraishi H*, et al.* Loss of SOCS3 gene expression converts STAT3 function from anti-apoptotic to pro-apoptotic. *J Biol Chem* 2006 Dec 1; **281**(48)**:** 36683-36690.

24. Roth W, Deussing J, Botchkarev VA, Pauly-Evers M, Saftig P, Hafner A*, et al.* Cathepsin L deficiency as molecular defect of furless: hyperproliferation of keratinocytes and pertubation of hair follicle cycling. *Faseb J* 2000 Oct; **14**(13)**:** 2075-2086.

25. Khaled WT, Read EK, Nicholson SE, Baxter FO, Brennan AJ, Came PJ*, et al.* The IL-4/IL-13/Stat6 signalling pathway promotes luminal mammary epithelial cell development. *Development* 2007 Aug; **134**(15)**:** 2739-2750.

26. Schmidt D, Wilson MD, Spyrou C, Brown GD, Hadfield J, Odom DT. ChIP-seq: using high-throughput sequencing to discover protein-DNA interactions. *Methods* 2009 Jul; **48**(3)**:** 240-248.

ACKNOWLEDGEMENTS

We thank Maximilian Blanck and Ivan Ferrer-Vicens for immunofluorescence studies, Helen Skelton for tissue histology and the Watson lab members for helpful discussions. This work was funded by BBSRC and MRC grants (BB/D012937/1 and MR/J001023/1) awarded to CJW, SP is the recipient of a Marie Curie IEF fellowship (EU Marie Curie grant no. 273365), KN was supported by a BBSRC CASE PhD studentship, HR is funded by a Cambridge Cancer Center PhD studentship and PAK is the recipient of a Trinity College fellowship. TR was supported by the Excellence Initiative of the German Federal and State Governments (EXC 294), and the Deutche Forschungsgemeinschaft SFB 850 project B7.

COMPETING FINANTIAL INTERESTS

The authors declare that they have no competing financial interests

FIGURE LEGENDS

Figure 1. p55α/p50α regulate cell death *in vivo*. (**a**) Immunoblot showing the complete deletion of p55α and p50α with retention of p85α in the *p55a*$^{-/-}$*/p50a*$^{-/-}$ mammary glands throughout involution. dL, days of lactation; hI, hours of involution. (**b**) Delay of mammary gland involution in *p55α*$^{-/-}$*/p50α*$^{-/-}$ mice, compared with *p55α*$^{+/+}$*/p50α*$^{+/+}$control mice, shown by haematoxylin and eosin (H&E)-stained sections. Scale bar, 200 μm. (**c**) Quantification of the area occupied by adipocytes, showing a significant difference in the percentage of adipose tissue at both 48h and 72h involution. The values represent means ± s.e.m. of two to four individual mice. (**d**) Quantification of luminal shed cells as detected in the H&E sections of 24h involution samples. The values represent means ± s.e.m. of three individual mice, with four fields per mouse counted. Black and white bars represent *p55α*$^{+/+}$*/p50α*$^{+/+}$ and *p55α*$^{-/-}$*/p50α*$^{-/-}$ glands respectively. Lac, lactation; Inv, involution. (**e**) Immunohistochemical analysis of the occurrence of cleaved caspase 3 in *p55α*$^{-/-}$*/p50α*$^{-/-}$ and control *p55α*$^{+/+}$*/p50α*$^{+/+}$ mice at 24h involution. Cleaved caspase-3 (c-C3)-positive shed cells can only be detected in the control mice. Scale bar, 100 μm. (* P <0.05, ** P<0.01, as determined by Student's t -test). (**f**) Immunoblot of cleaved-Caspase 3 (c-C3) in control (+/+) and *p55α*$^{-/-}$*/p50α*$^{-/-}$ mice (-/-) at 24h involution. E-cadherin is shown as loading control.

Figure 2. p55α/p50α regulate cathepsin L expression and cytosolic activity. (**a**) Rapid upregulation of cathepsin L at the onset of involution. Immunohistochemical analysis of cathepsin L (red) in control mice. 10 d Lac, 10 days lactation; 24, 48, 72, 96h Inv, hours of involution. Nuclei are stained with Hoechst. Scale bar, 20 μm. (**b**) Vesicles containing cathepsin L (red) but not cathepsin B (green) are shown by immunohistochemistry on 12h involution control samples. Insets of an example of vesicle containing only cathepsin L and one containing both cathpsin L and B are shown on the right side. Nuclei are stained with Hoechst. Scale bar, 20 μm. (**c**) Left, immunoblot showing decreased levels of cathepsin L (Ctsl) in the *p55α*$^{-/-}$*/p50α*$^{-/-}$ (-/-) mice as compared to control *p55α*$^{+/+}$*/p50α*$^{+/+}$ (+/+) mice. Three individual mice are shown per genotype at both 24h involution and 48h involution. Right, immunoblot of cytosolic extracts of three control and four *p55α*$^{-/-}$*/p50α*$^{-/-}$ mammary glands (sc; single

chain, dc; heavy chain of the double-chain form; both the single-chain and the double-chain form are active). β-actin is shown as loading control. (**d**) Reduced cytosolic activity of cathepsin L at 24h and 48h involution in *p55α*$^{-/-}$*/p50α*$^{-/-}$ glands when compared with controls, as opposed to unchanged cathepsin B activity shown by subcellular fractionation and subsequent cathepsin activity measurement. All values are means ± s**.**e.m. of at least three independent biological repeats. (**P*<0.05, as determined by Student's t -test).

Figure 3. p50α and p55α localize to the nuclei of mammary glands during involution and regulate transcription of a subset of genes. (**a**) Nuclear/cytosolic fractionation of mammary glands showing both cytosolic and nuclear localization of p50α, p55α and p85α. Lamin A/C and Tubulin are shown as loading and purity controls for the nuclear and cytosolic fraction, respectively. (**b**) Chromatin-enriched extracts of EpH4 mammary epithelial cells treated with vehicle (-OSM) or OSM (+OSM) showing the presence of phospho-Stat3 (p-Stat3) and p55α/p50α mainly in the chromatin-enriched fraction (ch) of the OSM-treated cells as opposed to the cytosolic (C) one whereas p85α is present on chromatin also in the control cells. t-Stat3, total Stat3. Histone H3 is shown as chromatin marker, whereas Tubulin shows the cytosolic fraction. Notably, Tubulin contamination in the chromatin fraction of the OSM treated cells is almost undetectable. (**c**) Quantitative real-time PCR relative to *cyclophilin a* of the following genes: *SAA2*, serum amyloid A 2; *Spp1*, secreted phosphoprotein 1; *Tlr2*, Toll-like receptor 2; *Slpi*, secretory leukocyte protease inhibitor; *Synpo*, synaptopodin. All results are means ± s.e.m. for three independent measurements and are representative of two independent biological repeats. (**d**) Quantitative real-time PCR relative to *cyclophilin a* of *Cathpsin L* and *B* and *Spi2A* expression at the indicated time points of mammary gland involution showing a decreased, although not significant, expression of Cathpsin L in the p50α/p55α$^{-/-}$ glands as compared to the controls. Results are means ± s.e.m. for at least four independent biological repeats.

Figure 4. Cathepsin L is an important mediator of mammary gland involution. (**a**) Immunoblot showing the complete deletion of cathepsin L in *cathepsin L*$^{-/-}$ (ctsl$^{-/-}$) glands compared to the controls (ctsl$^{+/+}$) at 72h involution. Tubulin is shown as loading control. (**b**) H&E sections and (**c**)

quantification of the percentage of area occupied by adipocytes at 72h involution clearly show the delay in involution in ctsl$^{-/-}$ mice compared to the controls. Quantification has been performed on two and three independent biological repeats for the control and the ctsl$^{-/-}$ mice, respectively. All values are means ± s.e.m. (**P<0.01, as determined by Student's t –test; scale bar, 100 μm). (**d**) Immunohistochemical analysis of the adipocytes (stained with perilipin, red) and epithelium (stainied with E-cadherin, green) in 72h of involution samples. Nuclei are stained with Hoechst. Scale bar, 100 μm.

FIGURES

Figure 1

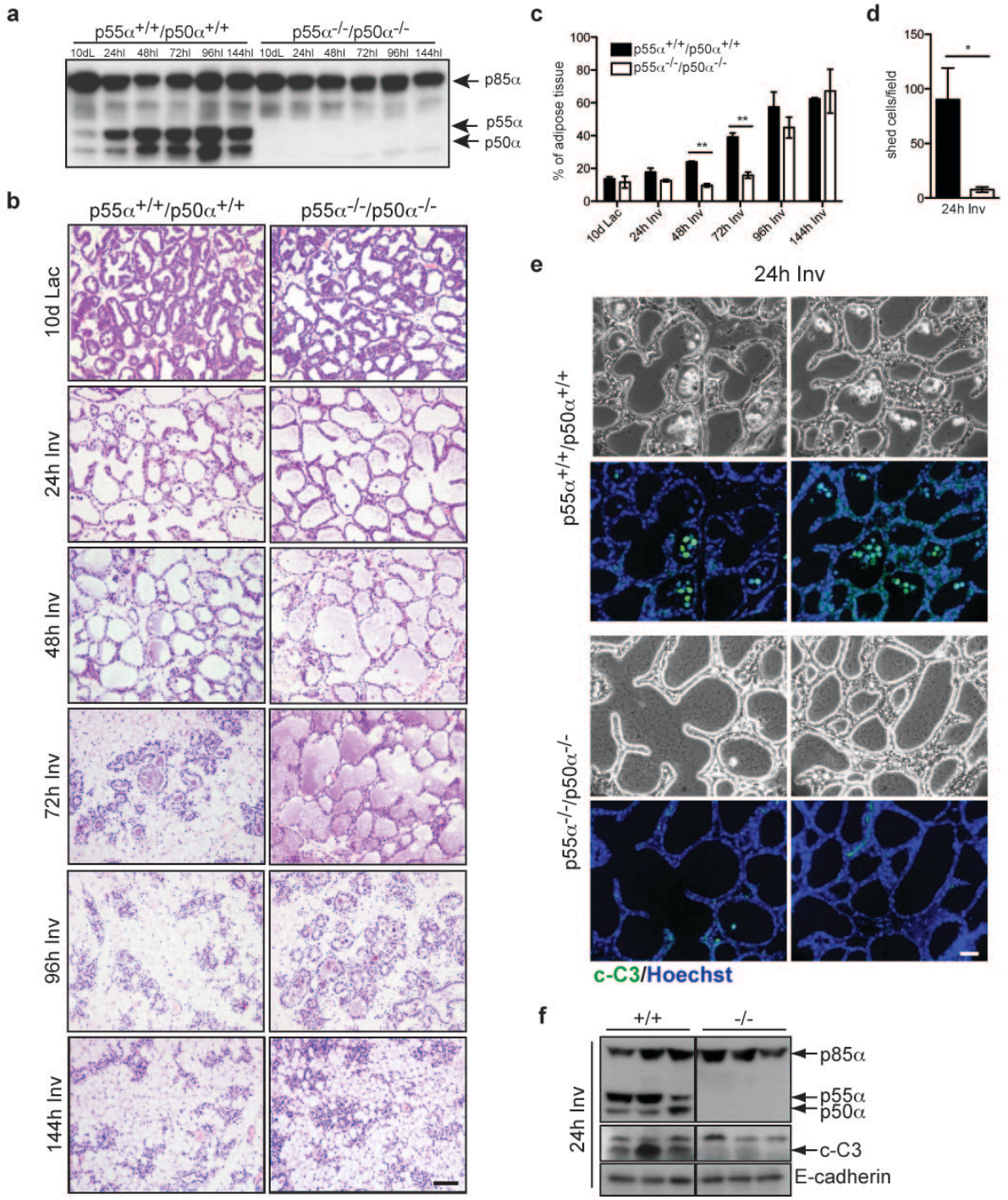

Figure 2

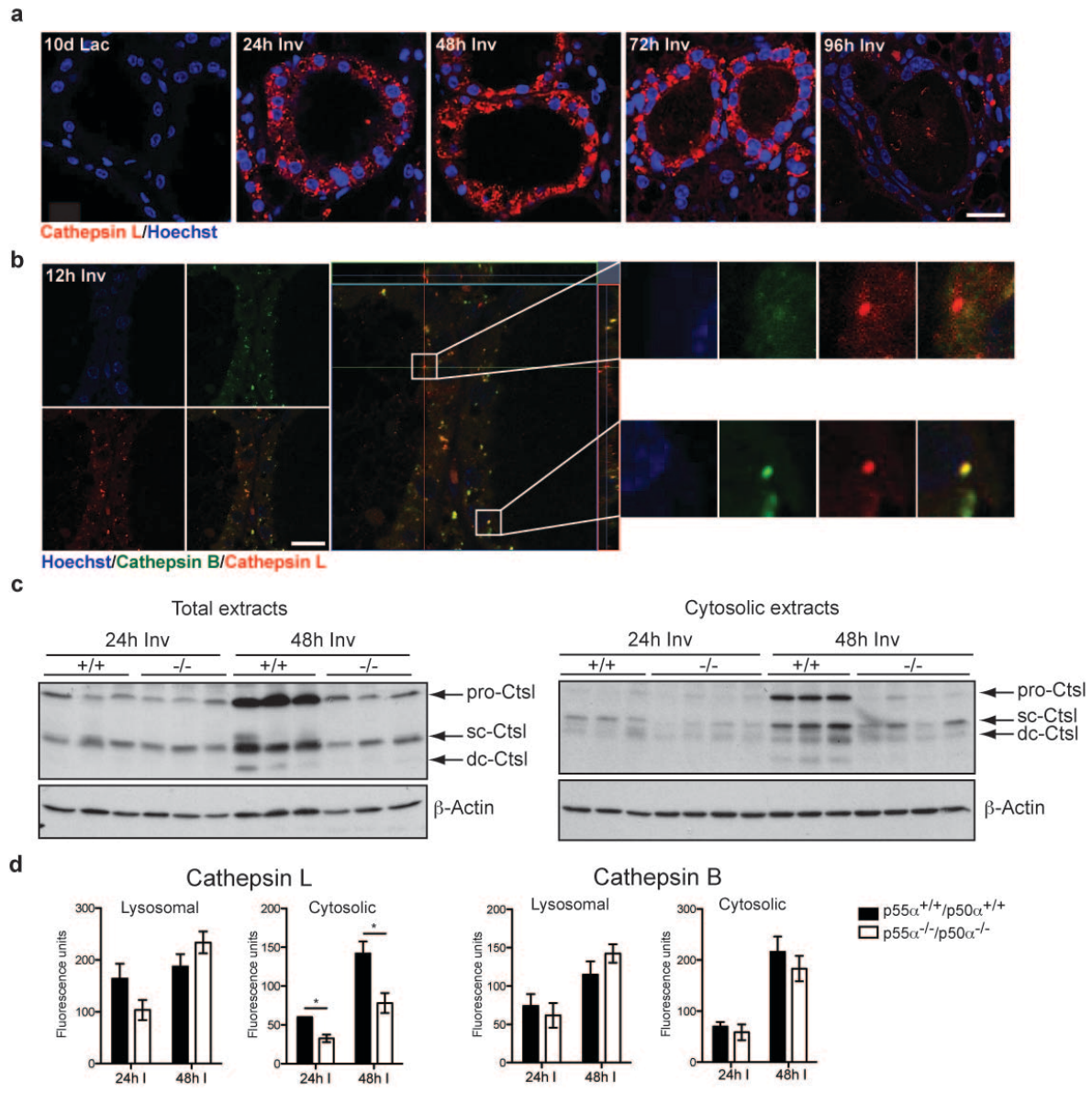
a
10d Lac
24h Inv
48h Inv
72h Inv
96h Inv
Cathepsin L/Hoechst
b
12h Inv
Hoechst/Cathepsin B/Cathepsin L
c
Total extracts
Cytosolic extracts
24h Inv
48h Inv
+/+
-/-
pro-Ctsl
sc-Ctsl
dc-Ctsl
β-Actin
d
Cathepsin L
Cathepsin B
Lysosomal
Cytosolic
Fluorescence units
24h I
48h I
p55α+/+/p50α+/+
p55α-/-/p50α-/-

Figure 3

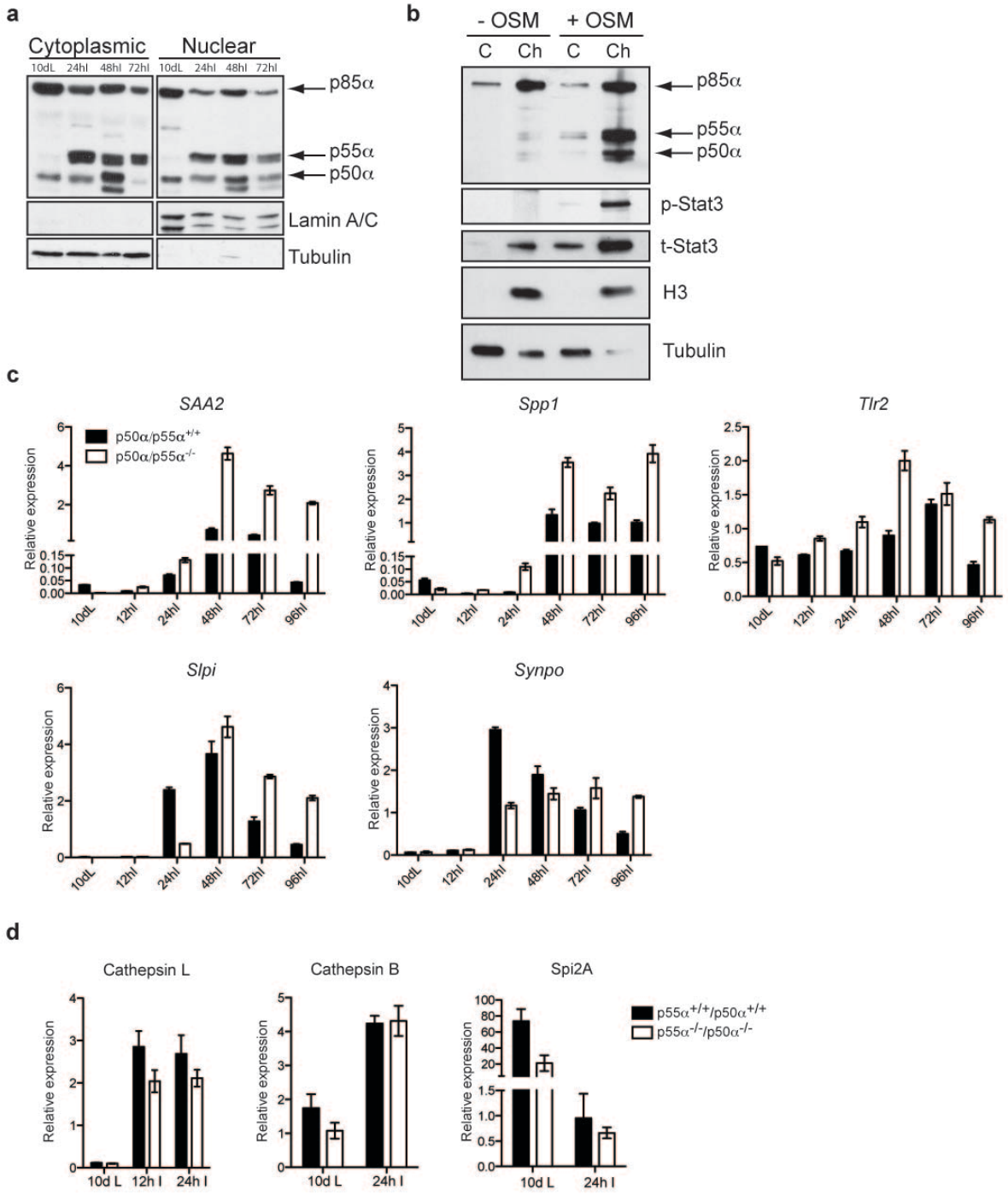
a
Cytoplasmic
Nuclear
10dL 24hl 48hl 72hl 10dL 24hl 48hl 72hl
p85α
p55α
p50α
Lamin A/C
Tubulin
b
- OSM
+ OSM
C Ch C Ch
p85α
p55α
p50α
p-Stat3
t-Stat3
H3
Tubulin
c
SAA2
Spp1
Tlr2
p50α/p55α+/+
p50α/p55α-/-
Relative expression
10dL 12hl 24hl 48hl 72hl 96hl
Slpi
Synpo
d
Cathepsin L
Cathepsin B
Spi2A
p55α+/+/p50α+/+
p55α-/-/p50α-/-
10d L 12h l 24h l
10d L 24h l

Figure 4

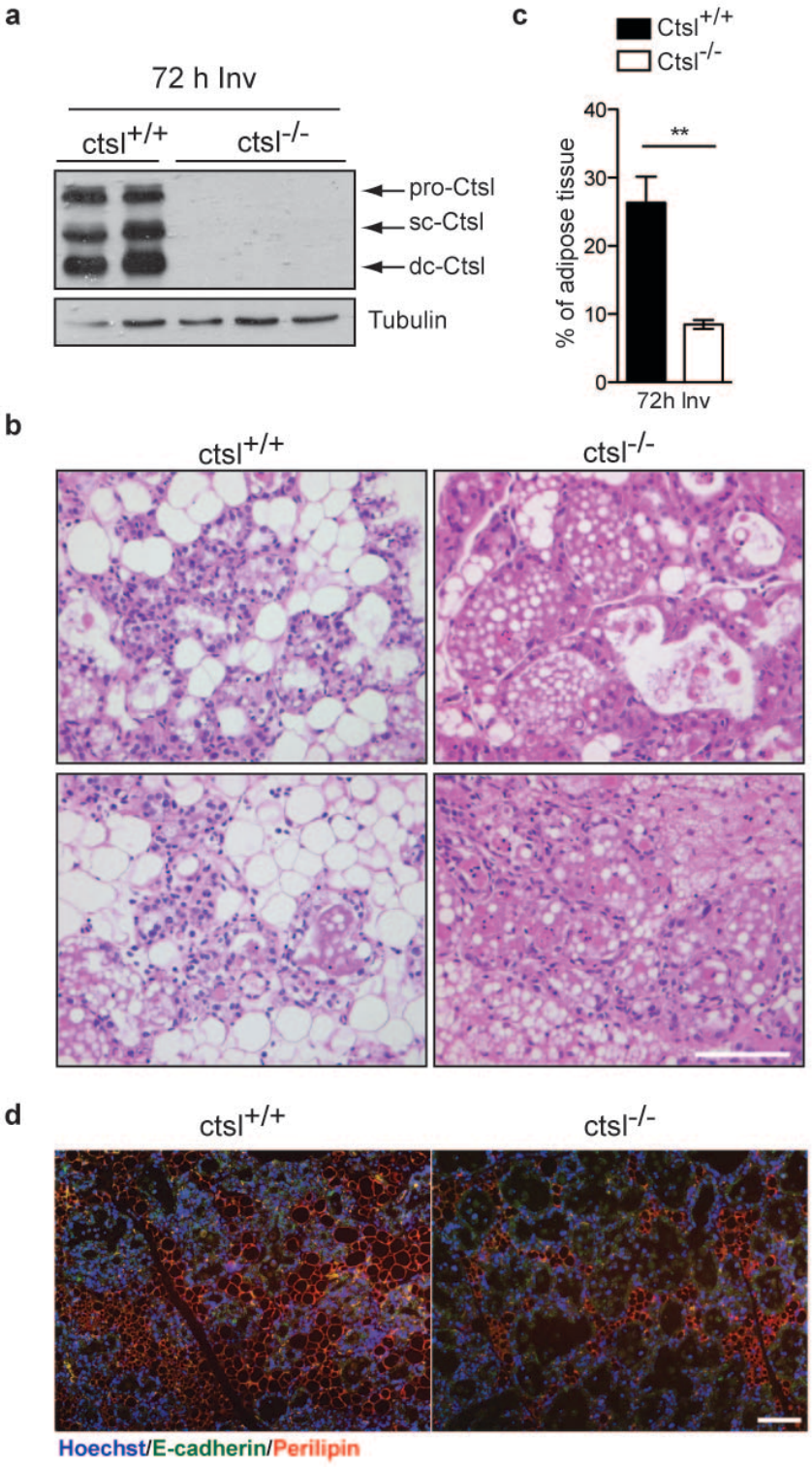
a
72 h Inv
ctsl+/+
ctsl-/-
pro-Ctsl
sc-Ctsl
dc-Ctsl
Tubulin
c
Ctsl+/+
Ctsl-/-
% of adipose tissue
40
30
20
10
0
**
72h Inv
b
ctsl+/+
ctsl-/-
d
ctsl+/+
ctsl-/-
Hoechst/E-cadherin/Perilipin